Polarized-Dependent IR ATR Study for the Structural Characterization of Solid-State Phosphonates: Case of Aluminum (4-Carboxyphenyl)methylphosphonate

Gérald Chaplais,† Jean Le Bideau,* Dominique Leclercq,* and André Vioux

UMR 5637 Chimie Moléculaire et Organisation du Solide, Université Montpellier II, case 007, Place E. Bataillon, F-34095 Montpellier Cedex 5, France

Received November 25, 2002. Revised Manuscript Received February 26, 2003

The hybrid organic−inorganic phosphonate Al(μ-OH)($O_3PCH_2C_6H_4COOH$)·H_2O has been structurally characterized by comparison of its polarized ATR-FTIR spectra, MAS NMR, and TGA analysis with those of Al(μ-OH)($O_3PCH_2C_6H_4Br$)·H_2O and Al(μ-OH)($O_3PCH_2C_6H_5$)·H_2O whose crystallographic structures are known. The polarized ATR (attenuated total reflection) IR study revealed the presence and orientation of selected bonds with respect to the sample holder. Moreover, for the three compounds, the polarized study allowed the identification of a symmetric CPO_3 vibration mode around 1050 cm^{-1}; usually, regular FTIR study of solid-state metallic phosphonates does not permit such precise attribution in this region of the IR spectrum. Polarized ATR FTIR spectroscopy, along with solid-state MAS NMR spectroscopy, appeared to be a very efficient tool for obtaining structural information on such solid-state hybrid compounds exhibiting highly anisotropic crystallites shapes.

1. Introduction

A growing interest has been devoted in recent years to the study of metal phosphonates.[1−4] Their properties show potential applications such as cation exchangers,[5] sorption,[6] catalysis,[7]sensors,[8] and nonlinear optics.[9] Metal phosphonates have been studied with divalent, trivalent, tetravalent, and hexavalent metals.[1,10−12] In the past few years, some studies have focused on aluminum phosphonates.[13−24] However, in this case, the synthesis of well-crystallized samples is often unsuccessful, so crystal structure determination is most often not possible, even with powder diffraction data.[22,23] To improve the characterization of metal phosphonates, specific NMR techniques have been developed,[25,26] and the combination of different spectroscopic methods has been used.[27,28] To our knowledge, the polarized attenuated total reflection (ATR) FTIR spectroscopy has not been used yet for bulk organic−inorganic solids, although it may be a promising technique for obtaining supplementary structural information. Indeed, polarized infrared radiation has been used extensively for the evaluation of molecular orientation and crystallinity in polymer films and performance of band assignments in oriented solids.[29−31]

* Corresponding authors.
† Current address: Max-Planck-Institut für Kohlenforschung, Kaiser-Wilhelm-Platz 1, Mülheim/Ruhr D-45470, Germany.

(1) Clearfield, A.; In *Progress in Organic Chemistry*; Karlin, K., D., Ed.; Wiley & Sons: Oxford, 1998; Vol. 47, pp 371−510.
(2) Alberti, G.; In *Comprehensive Supramolecular Chemistry*; Lehn, J. M., Ed.; Elsevier: New York, 1996; Vol. 7, pp 151−187.
(3) Thompson, M. E. *Chem. Mater.* **1994**, *6*, 1168.
(4) Cao, G.; Hong, H. G.; Mallouk, T. E. *Acc. Chem. Res.* **1992**, *25*, 420.
(5) Alberti, G. *Acc. Chem. Res.* **1978**, *11*, 163.
(6) Fredoueil, F.; Massiot, D.; Janvier, P.; Gingl, F.; Bujoli-Doeuff, M.; Evian, M.; Clearfield, A.; Bujoli, B. *Inorg. Chem.* **1999**, *38*, 1831.
(7) Deniaud D.; Schollorn B.; Mansuy D.; Rouxel J.; Battioni P.; Bujoli B. *Chem. Mater.* **1995**, *7*, 995.
(8) Alberti, G.; Casciola, M.; Polombari, R. *Solid State Ionics* **1992**, *52*, 291.
(9) Ungashe, S. B.; Wilson, W. L.; Katz, H. E.; Scheller, G. R.; Putvinski, T. M. *J. Am. Chem. Soc.* **1992**, *114*, 8717.
(10) Harrison, W. T. A.; Dussak, L. L.; Vaughey, J. T.; Vogt, T.; Jacobson, A. J. *J. Mater. Chem.* **1996**, *6*, 81.
(11) Aranda M. A. G.; Cabeza A.; Bruque S.; Poojary D. M.; Clearfield A. *Inorg. Chem.* **1998**, *37*, 1827−1832.
(12) Grohol, D.; Gingl, F.; Clearfield, A. *Inorg. Chem.* **1999**, *38*, 751.
(13) Maeda, K.; Kiyozumi, Y.; Mizukami, F. *Angew. Chem., Int. Ed. Engl.* **1994**, *33*, 2335.
(14) Maeda, K.; Akimoto, J.; Kiyozumi, Y.; Mizukami, F. *Angew. Chem., Int. Ed. Engl.* **1995**, *34*, 1199.
(15) Maeda, K.; Akimoto, J.; Kiyozumi, Y.; Mizukami, F. *J. Chem. Soc., Chem. Commun.* **1995**, 1033.
(16) Maeda, K.; Kiyozumi, Y.; Mizukami, F. *J. Phys. Chem. B* **1997**, *101*, 4402.
(17) Maeda, K.; Hashiguchi, Y.; Kiyozumi, Y.; Mizukami, F. *Bull. Chem. Soc. Jpn.* **1997**, *70*, 345.
(18) Haky, J. E.; Brady, J. B.; Dando, N.; Weaver, D. *Mater. Res. Bull.* **1996**, *32*, 297.
(19) Raki, L.; Detellier, C. *J. Chem. Soc., Chem. Commun.* **1996**, 2475.
(20) Hix, G. B.; Wragg, D. S.; Wright, P. A.; Morris, R. E. *J. Chem. Soc., Dalton Trans.* **1998**, 3359.
(21) Hix, G. B.; Carter, V. J.; Wragg, D. S.; Morris, R. E.; Wright, P. A. *J. Mater. Chem.* **1999**, *9*, 179.
(22) Cabeza, A.; Aranda, M. A. G.; Bruque, S.; Poojary, D. M.; Clearfield, A.; Sanz, J. *Inorg. Chem.* **1998**, *37*, 4168.
(23) Chaplais, G.; Le Bideau, J.; Leclercq, D.; Mutin, H.; Vioux, A. *J. Mater. Chem.* **2000**, *10*, 1593.
(24) Zakowsky, N.; Hix, G. B.; Morris, R. E. *J. Mater. Chem.* **2000**, *10*, 2375.
(25) Massiot, D.; Drumel, S.; Janvier, P.; Bujoli-Doeuff, M.; Bujoli, B. *Chem. Mater.* **1997**, *9*, 6.
(26) Bujoli-Doeuff, M.; Evain, M.; Fayon, F.; Alonso, B.; Massiot, D.; Bujoli, B. *Eur. J. Inorg. Chem.* **2000**, 2497.
(27) Drumel, S.; Janvier, P.; Bujoli-Doeuff, B.; Bujoli, B. *J. Mater. Chem.* **1996**, *6*, 1843.
(28) Chaplais, G.; Prouzet, E.; Flank, A. M.; Le Bideau, J. *New J. Chem.* **2001**, *25*, 1365.
(29) Francel, R. J. *J. Am. Chem. Soc.* **1952**, *74*, 1265.
(30) Ambrode, E. J.; Elliot, A.; Temple, R. B. *Nature* **1949**, *163*, 859.
(31) Colthup, N. B.; Daly, L. H.; Wiberley, S. E. *Introduction to Infrared and Raman Spectroscopy*; Academic Press: San Diego, 1990.

10.1021/cm0217304 CCC: $25.00
Published on Web 04/08/2003

Scheme 1. Schematic Representation of the Orientation of Layered Particles on the Surface of the ATR Sample Holder (ZnSe Crystal)

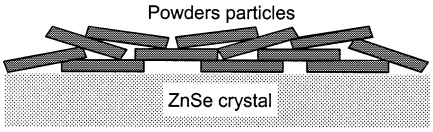

In the ATR technique, the infrared beam is transmitted through an elongated crystal (the ATR sample holder, here, a ZnSe crystal) by reflecting several times the beam from the surfaces of the ZnSe crystal at an angle greater than the critical angle for the total internal reflection. The total internal reflection of the infrared beam at the ZnSe/sample interface produces an evanescent wave that propagates in the sample, through some micrometers for our samples; a bond that exhibits a dipolar vibration mode that absorbs in the infrared region will attenuate the reflected beam and absorbance due to this bond will be observed.[32] Adding polarization of the internally reflected beam results in the production of an evanescent wave that has electric field either parallel to the surface of the sample holder (P_0 polarization) or perpendicular to it, which produces a major component perpendicular to the surface (P_{90}). Comparing the absorbance of a vibration mode with each polarization allows determination of the orientation of the mode with respect to the sample holder surface. Powders formed by platelike crystallites, even if the crystallites size is small, can be preferentially oriented by deposition onto the sample holder. We obtain a high statistical orientation as shown in Scheme 1, and the variation of absorbance with the angle of polarization for some vibration modes is clear enough to determine if these vibration modes are parallel or perpendicular to the sample holder surface, that is, to the plane of the sample's layers. As a result, structural information about initially structurally unknown compounds could be obtained by combination of MAS NMR and polarized ATR-FTIR spectroscopy.

The aim of this paper is to highlight this possibility by studying with polarized ATR-FTIR spectroscopy two structurally known lamellar compounds, Al(μ-OH)($O_3PCH_2C_6H_4Br$)·H_2O[23] (**1**) and Al(μ-OH)($O_3PCH_2C_6H_5$)·H_2O[24] (**2**), and a structurally unknown compound, Al(μ-OH)($O_3PCH_2C_6H_4COOH$)·H_2O (**3**), whose TGA, ^{31}P and ^{27}Al MAS NMR, and FTIR spectra suggest that it belongs to the same structural type.

2. Experimental Section

Aluminum sulfate octadecahydrate 98+% and triethyl phosphite were purchased from Aldrich and 4-(bromomethyl)-benzoic acid from Lancaster. Elemental analyses were performed by the "Centre National d'Analyse du CNRS", Vernaison, France. ^{1}H NMR (200 MHz), ^{13}C NMR (50.28 MHz), and ^{31}P NMR (81.01 MHz) spectra were recorded on a Bruker ADVANCE DPX 200 spectrometer and internally referenced to tetramethylsilane (^{1}H, ^{13}C) or to 85% phosphoric acid (^{31}P). A proton decoupling was carried out for ^{13}C and ^{31}P NMR spectroscopy. A ^{13}C CP MAS (75.75 MHz) spectrum was recorded on a Bruker DPX-300 spectrometer, with a 4-mm rotor and a spinning rate of 10 kHz, and referenced to tetramethylsilane. ^{31}P MAS NMR (80.96 MHz) spectra were recorded on a Bruker ASX-200 spectrometer, by proton decoupling and with a 4-mm rotor, referenced to 85% phosphoric acid, and a spinning rate from 1 to 6 kHz that allowed the determination of the shielding tensor asymmetry κ (skew)[33,34] via the fit of the signal using the Bruker Win-Mass software. ^{27}Al MAS NMR (104.26 MHz) spectra were recorded on a Bruker ASX-400 spectrometer, with a 4-mm rotor and a spinning rate of 12 kHz and referenced to a 1.5 M aqueous solution of aluminum chloride hexahydrate. All isotropic chemical shifts for the aluminum nucleus were obtained via a fit of the signal using the Bruker Win-Fit software. Thermogravimetric analyses were performed on a NETZSCH 409 thermo balance, under air flow, at 5 °C min^{-1}. FTIR spectra were performed on a Perkin-Elmer 2000 spectrometer by using KBr as matrix pellets. Polarized ATR FTIR spectra were performed on the same spectrometer, using a Graseby Specac P/N 12950 polarizer. The samples were deposited onto a ZnSe crystal and pressed to afford a high preferential orientation and to optimize the contact of the sample onto the ZnSe crystal surface. Aluminum bromobenzylphosphonate Al(μ-OH)($O_3PCH_2C_6H_4Br$)·H_2O (**1**) and aluminum benzylphosphonate Al(μ-OH)($O_3PCH_2C_6H_5$)·H_2O (**2**) were prepared as previously reported.[23,24] Aluminum carboxybenzylphosphonate Al(μ-OH)-($O_3PCH_2C_6H_4COOH$)·H_2O (**3**) and its precursors were prepared according to Scheme 2.

Preparation of 4-(Diethoxyphosphorylmethyl)benzoic Acid Ethyl Ester (4). A mixture of 100 mL of triethyl phosphite (0.58 mol) and 12.83 g of 4-(bromomethyl)benzoic acid (0.60 mol) was heated for 20 h at 140 °C. After distillation ($bp_{0.1}$ = 137 °C), 15.8 g (0.53 mol) of a clear liquid was obtained (yield: 91%). ^{1}H NMR ($CDCl_3$, δ/ppm): 1.28 (t, $POCH_2CH_3$, $^3J_{HH}$ = 7.1 Hz), 1.43 (t, $COCH_2CH_3$, $^3J_{HH}$ = 7.1 Hz), 3.24 (d, PCH_2, $^2J_{HP}$ = 22.1 Hz), 4.06 (m, $POCH_2CH_3$), 4.40 (q, $COCH_2$-CH_3, $^3J_{HH}$ = 7.1 Hz), 7.41 (m, C(O)$C_{ar.}C_{ar.}$H), 8.03 (m, C(O)-$C_{ar.}C_{ar.}C_{ar.}$H). ^{13}C {^{1}H} NMR ($CDCl_3$, δ/ppm): 14.73 (s, $COCH_2$-CH_3), 16.77 (d, $POCH_2CH_3$, $^3J_{CP}$ = 6.0 Hz), 34.42 (d, PCH_2, $^1J_{CP}$ = 137.5 Hz), 61.36 (s, $COCH_2CH_3$), 62.68 (d, $POCH_2CH_3$, $^2J_{CP}$ = 6.8 Hz), 129.58 (d, C(O)$C_{ar.}$, $^5J_{CP}$ = 3.5 Hz), 130.12 (s, C(O)-$C_{ar.}C_{ar.}$), 130.21 (d, $PCH_2C_{ar.}C_{ar.}$, $^3J_{CP}$ = 2.8 Hz), 137.44 (d, $PCH_2C_{ar.}$, $^2J_{CP}$ = 9.1 Hz), 166.81 (d, C=O, $^6J_{CP}$ = 1.6 Hz). ^{31}P {^{1}H} NMR ($CDCl_3$, δ/ppm): 26.5.

Preparation of 4-(Phosphonomethyl)benzoic Acid (5). Five grams of **4** (16.7 mmol) was refluxed for 20 h in 50 mL of 32% hydrogen chloride, leading to a precipitate which was filtrated and dried for 12 h under vacuum to give 3.33 g (15.4 mmol) of a white powder (yield: 92%). mp = 282−285 °C. ^{1}H NMR (DMSO-d_6, δ/ppm): 3.07 (d, PCH_2, $^2J_{HP}$ = 21.8 Hz), 7.38 (m, $PCH_2C_{ar.}C_{ar.}H$), 7.87 (m, C(O)$C_{ar.}C_{ar.}H$). ^{13}C {^{1}H} NMR (DMSO-d_6, δ/ppm): 36.47 (d, PCH_2, $^1J_{CP}$ = 130.8 Hz), 129.30 (d, C(O)$C_{ar.}$, $^5J_{CP}$ = 3.3 Hz), 129.91 (d, C(O)$C_{ar.}C_{ar.}$, $^4J_{CP}$ = 2.7 Hz), 130.76 (d, $PCH_2C_{ar.}C_{ar.}$, $^3J_{CP}$ = 6.1 Hz), 140.68 (d, $PCH_2C_{ar.}$, $^2J_{CP}$ = 8.7 Hz), 168.13 (s, C=O). ^{13}C CPMAS NMR (δ/ppm): 31.3 (d, PCH_2, $^1J_{CP}$ = 134.3 Hz), 129.0 (s, C(O)$C_{ar.}$), 132.5 (s, C(O)$C_{ar.}C_{ar.}$ and $PCH_2C_{ar.}C_{ar.}$), 138.78 (s, $PCH_2C_{ar.}$), 172.43 (s, C=O). ^{31}P {^{1}H} NMR (DMSO-d_6, δ/ppm): 21.3. ^{31}P {^{1}H} MAS NMR, (δ/ppm): 30.4.

Preparation of Al(μ-OH)($O_3PCH_2C_6H_4COOH$)·H_2O (3). **5** (1.52 g, 7.0 mmol) and aluminum sulfate octadecahydrate (0.59 g, 0.9 mmol) were suspended in 20 mL of water (Al/P/H_2O: 0.25/1/158) and transferred to a Pyrex tube, which was sealed and heated for 4 days at 180 °C. After 8 h of controlled cooling, the white crystalline powder was filtrated, washed with water (200 mL) and ethanol (400 mL), and dried at room temperature for 24 h (0.45 g, 1.6 mmol, yield: 89%). Anal. Found (calcd): Al, 9.55 (9.77); P, 11.25 (11.21); C, 34.51 (34.80); H, 3.73 (3.65).

3. Results and Discussion

3.1. Crystallography. Crystallographic structures of compounds **1** and **2** have been determined.[23,24] They

(32) Mirabella, F. M.; Harrick, N. J. *Internal Reflection Spectroscopy: Review and Supplement*; Harrick Scientific Corporation: New York, 1985.

(33) Mason, J. *J. Nucl. Magn. Reson.* **1993**, *2*, 285.

(34) Jameson, C. J. *Solid State NMR* **1998**, *11*, 265.

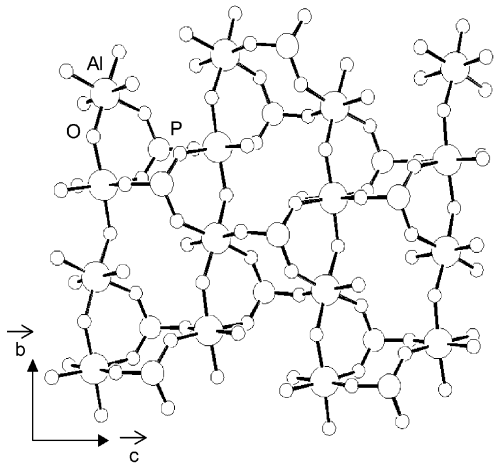

Figure 1. View of an inorganic layer of Al(μ-OH)($O_3PCH_2C_6H_4$-Br)·H_2O showing the Al-μOH−Al chains along the *b* axis (carbon and bromine atoms have been removed for clarity).

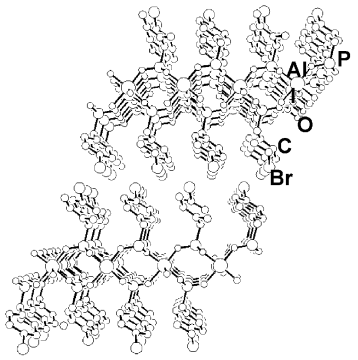

Figure 2. Perspective view of Al(μ-OH)($O_3PCH_2C_6H_4Br$)·H_2O showing the pendant bromobenzyl groups between the inorganic layers.

exhibit a bidimensional arrangement; the inorganic layers consist of aluminum atoms in an octahedral environment of oxygen atoms, sharing three corners with three tetrahedral environments around the phosphorus atoms, two corners with two neighboring octahedrons of aluminum atoms through μ-OH bridges, and the last corner occupied by an oxygen atom of a water molecule. The μ-OH bridges expand down the *b* axis, thus making an Al−OH−Al chain (Figure 1). Neighboring chains within a layer are bridged by phosphorus tetrahedrons through Al−O−P−O−Al linkage sequences. Each of the three phosphonato oxygen atoms is bonded to only one aluminum atom. The fourth corner of the phosphorus environment is occupied by a carbon atom that connects with a covalent bond the inorganic layer to the organic part which points between two layers; the P−C bond is quasi-perpendicular to the layer (Figure 2). Due to the sp^3 carbon atom, which separates

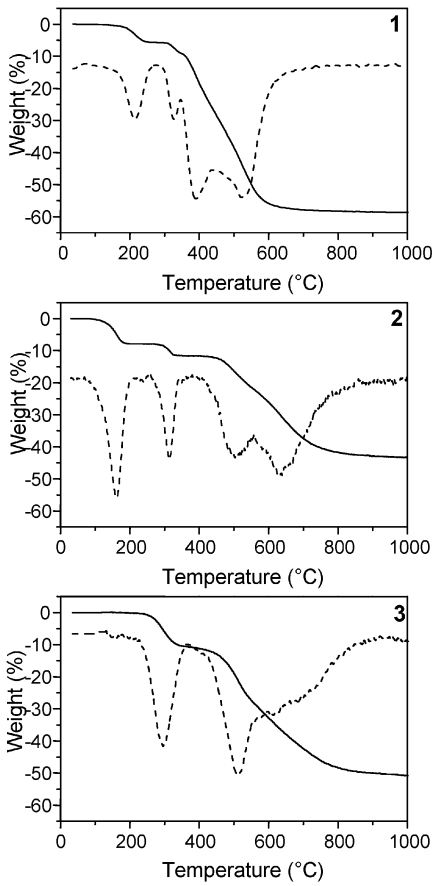

Figure 3. Thermogravimetric (solid) and derivative (dotted) curves for 1, 2, and 3.

the phosphorus atom from the phenyl ring, there is a 45° dihedral angle between the inorganic plane and the phenyl plane. In the case of compound **3**, the powder X-ray diffraction did not allow us to obtain reliable cell parameters; nevertheless, the interlamellar distance is found at 1.512 nm, which is very close to the interlamellar distance found for the bromobenzyl derivative **1** (1.513 nm) and significantly higher than that found for the benzyl derivative **2** (1.369 nm).

3.2. Thermal Analysis. For **1** and **2**, thermogravimetric analyses reveal two mass losses (Figure 3): for **1**, a 5.7% mass loss at 215 °C (theoretical mass loss for one water molecule: 5.8%) and a 3.1% mass loss at 332 °C (theoretical for $0.5H_2O$: 3.1%); for **2**, a 7.5% mass loss at 160 °C (theoretical 7.8%) and a 4.0% mass loss at 307°C (theoretical 4.2%). For **3**, only one mass loss of 10.2% is observed at 298 °C (theoretical mass loss for 1.5 water molecules: 9.8%) (Figure 3). The three compounds show the same thermal behavior, although the two first phenomena appear together for **3**: loss of one water molecule, condensation of the μ-OH groups

Scheme 2. Synthesis of 3

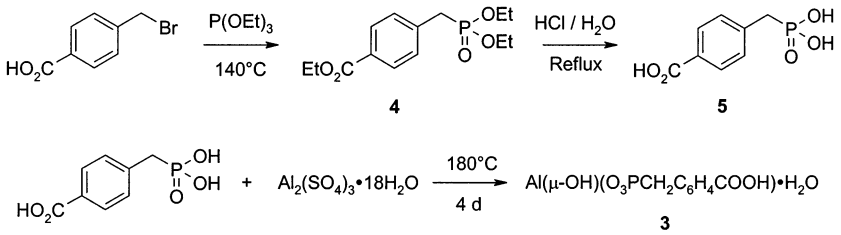

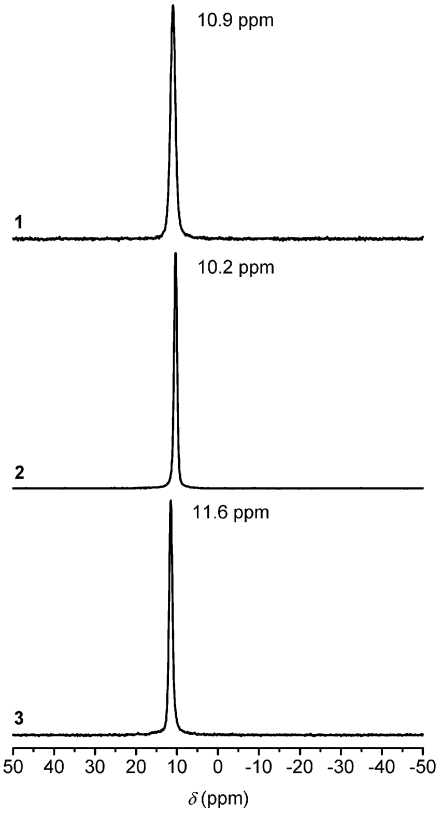

Figure 4. ^{31}P MAS NMR spectra for **1**, **2**, and **3**.

Table 1. ^{31}P and ^{27}Al MAS NMR Parameters: κ Shielding Tensor Asymmetry; C_Q Quadrupolar Coupling Constant; η_Q Asymmetry Factor.

	^{31}P			^{27}Al		
	δ (ppm)	κ	connectivity	δ_{iso} (ppm)	C_Q (kHz)	η_Q
1	10.9	−0.20	111	1.1	6520	0.74
2	10.2	−0.20	111	0.5	6420	0.74
3	11.6	−0.16	111	−2.4	4064	0.25

(two neighboring μ-OH groups for one water molecule) with the release of 0.5 water molecule per formula unit, and finally degradation of the organic groups to give $AlPO_4$ as the final residue obtained at 1200 °C and identified from PXRD. The temperature of dehydration increases in the series H < Br < COOH, that is, increases with the size of the para substituent, while the temperature of hydroxyl groups condensation is nearly the same (from 298 to 332 °C).

3.3. NMR Spectroscopic Study. The ^{31}P MAS NMR spectra of the three titled compounds show only one signal for each compound with very close isotropic chemical shifts, between 10.2 and 11.6 ppm (Figure 4). The values of the shielding tensor asymmetry (κ) are also very close to each other, thus showing that the connectivity of the phosphonato group (i.e., the number of metal atoms bonded to each phosphonato oxygen atom) is constant (Table 1).[25] The narrow distributions of the ^{31}P NMR chemical shifts and of the shielding tensor asymmetry (κ) indicate that the distances and angles in the environment of the phosphorus atoms were highly similar for the three compounds.[16]

The ^{27}Al MAS NMR spectra exhibit broad and asymmetric signals due to the quadrupolar effect of the ^{27}Al nucleus (Figure 5). Fitting of the signals showed only one isotropic chemical shift for each compound, from 1.1 to −2.4 ppm, which corresponds to an octahedral environment (Table 1). The lower value of the quadrupolar coupling constant C_Q and asymmetry factor η_Q of **3** might correspond to a lower distortion of the oxygen atoms octahedron around the aluminum atom.

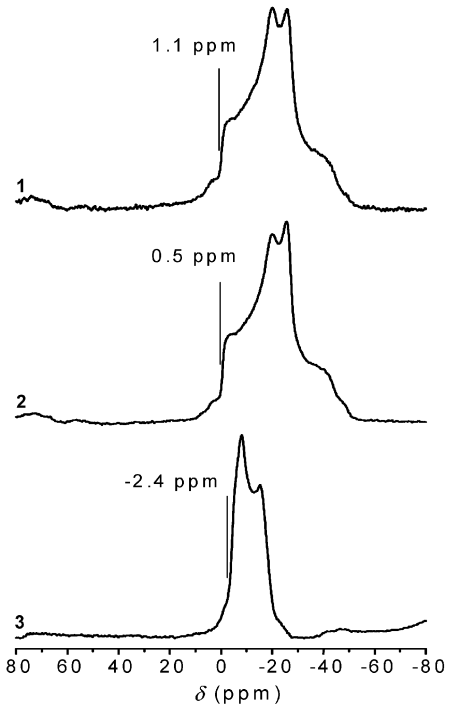

Figure 5. ^{27}Al MAS NMR spectra for **1**, **2**, and **3**.

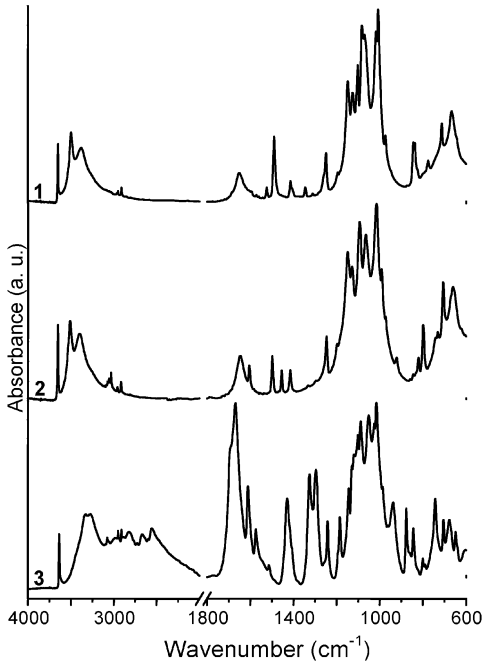

Figure 6. FTIR spectra for **1**, **2**, and **3**.

3.4. FTIR Spectroscopic Study. The IR spectra of the three compounds performed in KBr pellets are shown in Figure 6. The assignments of the absorption bands are based on literature values.[31] A medium and sharp band corresponding to the stretching vibration of μ-OH appeared at 3651, 3654, and 3635 cm^{-1} for **1**, **2**, and **3**, respectively. Two broad bands are related to the stretching vibration of the O−H bonds of coordi-

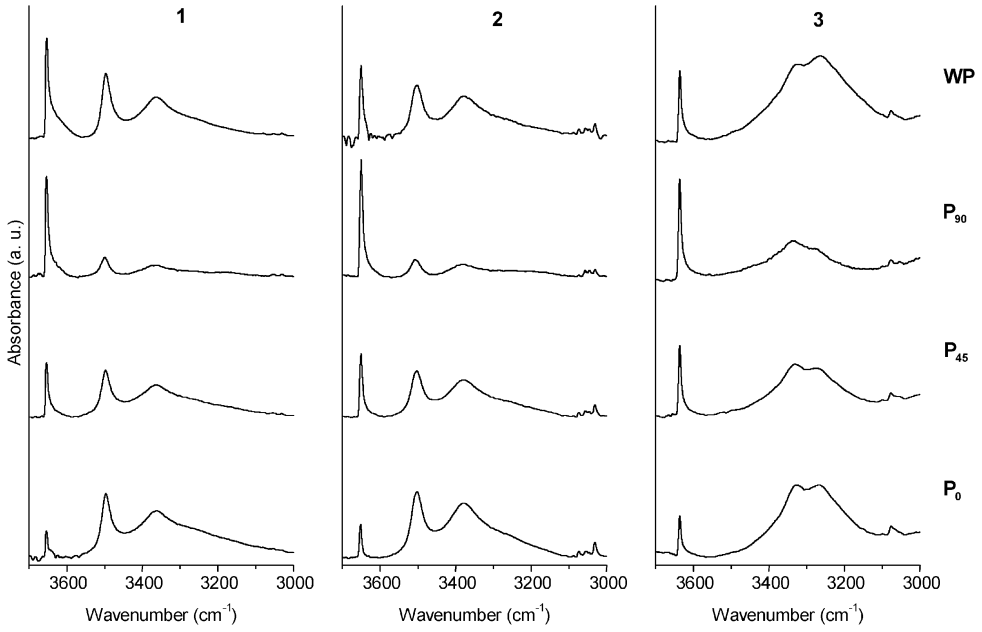

Figure 7. Polarized ATR-FTIR spectra for **1**, **2**, and **3** between 3000 and 3700 cm^{-1}.

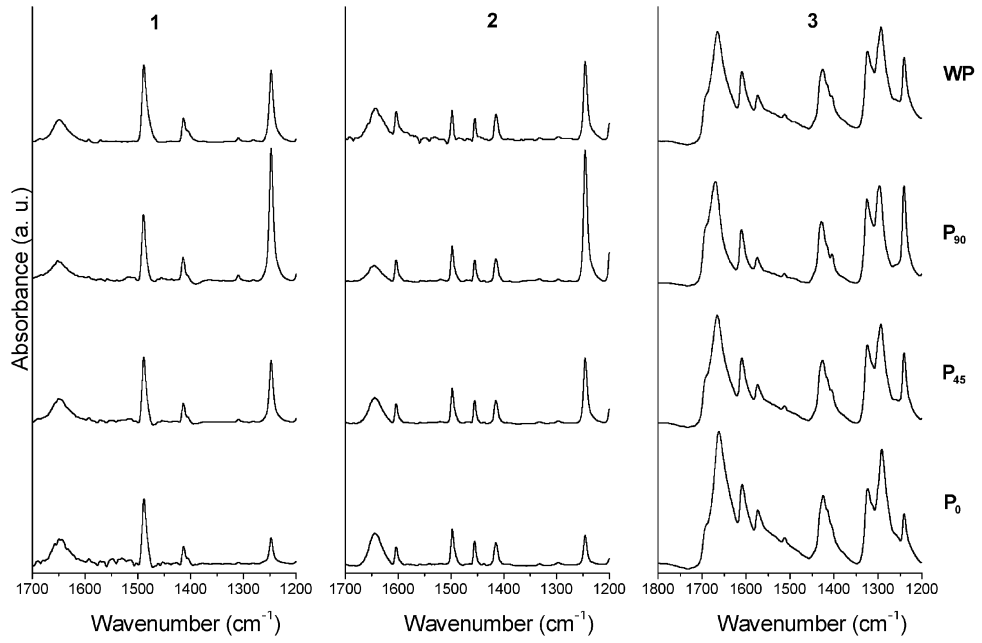

Figure 8. Polarized ATR-FTIR spectra for **1**, **2**, and **3** between 1200 and 1800 cm^{-1}.

nated water between 3100 and 3500 cm^{-1}. The bending vibration of water appears at 1646 and 1643 cm^{-1} for **1** and **2**, respectively. For **3**, it is hidden by the stretching vibration band of the C═O bond of the carboxylic group at 1665 cm^{-1}. The weak stretching vibration bands of the C−H bonds of the aromatic ring are observed between 3015 and 3100 cm^{-1} for **1** and **2** and around 3075 cm^{-1} for **3**. The same group presents medium intensity bands for the three compounds between 1400 and 1600 cm^{-1} due to stretching vibrations ν(C═C). The stretching vibration bands of the CH_2 groups appear between 2910 and 2957 cm^{-1}. The strong stretching vibration bands of the phosphonato group PO_3 are situated between 900 and 1200 cm^{-1}. Supplementary bands for **3** are ascribed to the carboxylic group: ν(O−H) at 3000 cm^{-1}, overtone bands at 2663 and 2554 cm^{-1}, δ_p(O−H) at 1429 cm^{-1}, ν(C−O) at 1294 cm^{-1}, and δ_{op}-(O−H) at 937 cm^{-1}.

3.5. Polarized ATR FTIR Study. All previous observations evidence for compound **3** a similar structural organization as for **1** and **2**. Nevertheless, polarized ATR FTIR is shown to bring some more very precise structural evidence on the isostructurality of the inorganic layers of the three compounds. Four different measurements are reported herein: a first with a polarization parallel to the ZnSe crystal plane (P_0), a second with a polarization with a 45° rotation respective to the first one (P_{45}), a third with a 90° rotation, that is, with a major component perpendicular to the ZnSe crystal plane (P_{90}), and a fourth without any polarization (WP).

The first wavenumber region presented ranges from 3000 to 3700 cm^{-1} (Figure 7). The relative intensity of the ν(μ-O−H) stretching bands around 3650 cm^{-1} for

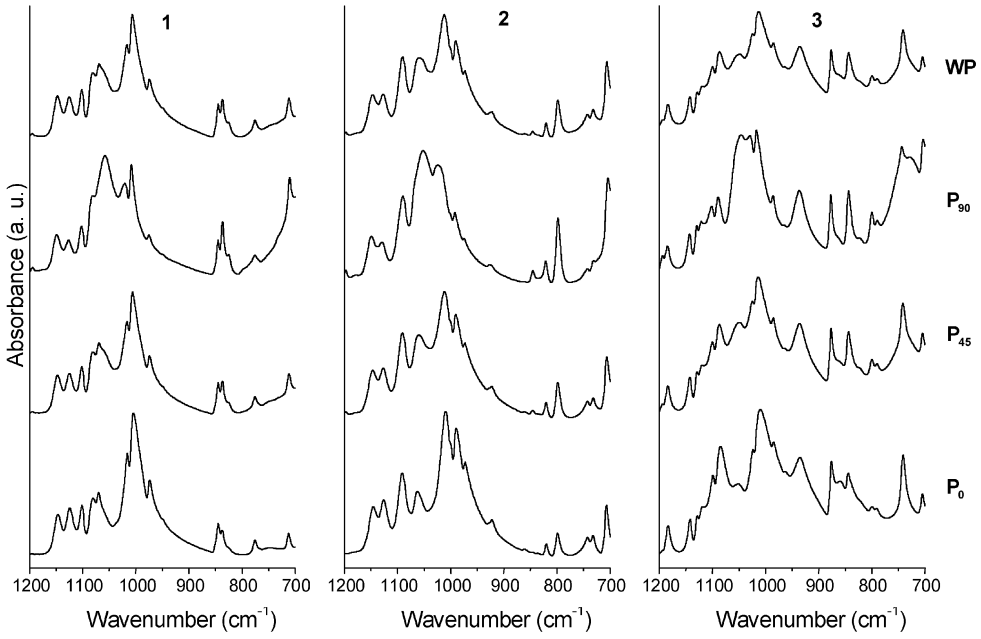

Figure 9. Polarized ATR-FTIR spectra for **1**, **2**, and **3** between 700 and 1200 cm^{-1}.

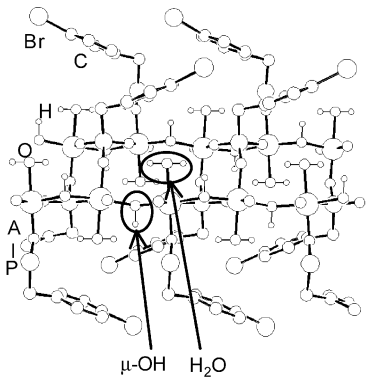

Figure 10. Schematic view down the *c* axis of an inorganic layer of Al(μ-OH)($O_3PCH_2C_6H_4Br$)·H_2O; the hydrogen atoms have been artificially added on the oxygen atoms of the water molecules and on the bridging oxygen atoms (μ-OH).

the three compounds increases when the polarization varied from P_0 to P_{90}, thus showing that the μ-O−H bond should be rather perpendicular to the lamellar plane for each aluminophosphonate. The decrease of the relative intensity of the ν(O−H) stretching bands of H_2O (from P_0 to P_{90}) indicates that the OH bonds of the water molecule should be rather parallel to the inorganic plane. This is confirmed by the relative decrease of the δ_p(O−H) deformation bands of water at 1650 cm^{-1} when the polarization varied from P_0 to P_{90} in Figure 8 (more easily observable for **1** and **2**). The orientations of the μ-O−H bonds and of the O−H bonds of the water molecules are schematically shown in Figure 10, on which protons have been added to the structure determined from powder diffraction for **1**.

For **1** and **2**, no modification of the intensity of the bands at 1410 and 1480 cm^{-1} (Figure 8) attributed to the stretching vibration of the carbon−carbon bonds from the aromatic rings appears, which is coherent with the intermediate dihedral angle between the inorganic layers and the phenyl rings planes.[23,24] The band near 1250 cm^{-1} increased when the polarization varied from P_0 to P_{90}, showing that the corresponding bond is perpendicular to the inorganic plane. The wavenumber of this band is very close to that attributed to ν(P−CH_3).[10,35] Moreover, the structure of **1** shows that the P−CH_2 bond is nearly perpendicular to the inorganic plane angles. This evidences that this band is due to the P−CH_2 stretching vibration. For the compound **3**, the intensity of the ν(C═O) band of the carboxylic group at 1665 cm^{-1} decreases slightly when the polarization varied from P_0 to P_{90}, indicating that this vibration is oriented rather parallel to the inorganic plan. Moreover, the low value of this vibration indicates the existence of hydrogen bonds between carboxylic acid functions, which is confirmed by the presence of overtone bands at 2663 and 2554 cm^{-1} (Figure 6).[31] In the P−O stretching region (Figure 9), the band close to 1050 cm^{-1}, which is weak without polarization, increases drastically when the polarization varied from P_0 to P_{90}. Consequently, the strong bands at 1058 cm^{-1}(**1**), 1052 cm^{-1} (**2**), and 1047 cm^{-1} (**3**) observed for P_{90} should be assigned to a vibration mode of the CPO_3^{2-} group. The drastic increase in the relative intensity of this band evidence a vibrating dipole, whose axis is perpendicular to the layer. The most likely modes that could be associated with such a dipole are symmetric modes: an asymmetric mode of a XAY_3 molecule cannot result in a strong dipole variation along the X−A direction, that is, along the C−P direction, perpendicular to the layer.

Table 2. Orientation of Vibration Modes Respective to the Inorganic Plane, Perpendicular (⊥) or Parallel (//) to the Inorganic Plane.

groups	1		2		3	
μ-OH	3653 cm^{-1}	⊥	3651 cm^{-1}	⊥	3635 cm^{-1}	⊥
	3497 cm^{-1}	//	3502 cm^{-1}	//	3322 cm^{-1}	//
H_2O	3363 cm^{-1}	//	3377 cm^{-1}	//	3264 cm^{-1}	//
	1646 cm^{-1}	//	1643 cm^{-1}	//	1650 cm^{-1}	//
COOH					1665 cm^{-1}	//
P−CH_2	1247 cm^{-1}	⊥	1245 cm^{-1}	⊥	1241 cm^{-1}	⊥
PO_3	1058 cm^{-1}	⊥	1052 cm^{-1}	⊥	1047 cm^{-1}	⊥

(35) Harrison, W. T. A.; Dussak, L. L.; Jacobson, A. J. *Inorg. Chem.* **1996**, *35*, 1461.

Thus, two symmetric modes might be at the origin of this band. The first most likely mode is the symmetric stretching of the three P−O bonds, which results in a dipole variation along the P−C direction. The second most likely mode is the symmetric bending of the three P−O bonds, also called umbrella-like bending, which gives the same result.

To our knowledge, such precise assignment in this range has not been carried out yet for such solid-state hybrid organic−inorganic materials.

The main bands and their orientation to the plane are reported in Table 2.

4. Conclusion

The polarized ATR FTIR spectroscopy study of the structurally known **1** and **2** shows relative increases and decreases of the intensities of the absorption bands with respect to the orientation of the polarization of the IR beam. The results obtained by this method are in a very good agreement with the crystallographic data and allowed to ascertain the isostructurality of the inorganic layers of **1**, **2**, and **3**. On one hand, polarization allowed us to determine the orientation of the μ-O−H bonds and of the O−H bonds from the coordinated water molecule for the two structurally known compounds **1** and **2**, which is often not straightforward from an X-ray study. On the other hand, about the unknown compound **3**, polarization permitted us to obtain precise structural information on the orientation of the C═O bonds. The μ-O−H and the O−H bonds of the water molecule for **3** were shown to have the same orientation as in **1** and **2**. Moreover, for all three compounds, polarization allowed the identification of the band around 1050 cm^{-1} in the P−O region with only two possible symmetric vibration modes. By crossing these results with NMR spectroscopy, we have shown unambiguously that **3** Al(μ-OH)($O_3PCH_2C_6H_4COOH$)·H_2O possesses the same structure of the inorganic layers as **1**, Al(μ-OH)($O_3PCH_2C_6H_5$)·H_2O, and **2**, Al(μ-OH)($O_3PCH_2C_6H_4Br$)·H_2O. The polarized ATR FTIR technique appears to be very pertinent for obtaining structural information in hybrid organic−inorganic solids provided that a crystallites shape anisotropy allows preferred orientation of the sample deposited on the ATR sample holder.

CM0217304